Geodesy and Geodynamics 2013,4(1):7 - 15

http://www.jgg09.com
Doi:10.3724/SP.J.1246.2013.01007

Tidal characteristics near the Chinese Zhongshan Station in Prydz Bay, East Antarctica

Huang Jifeng[1,2], E Dongchen[1,2] and Zhang Shengkai[1,2]

[1] *Chinese Antarctic Center of Surveying and Mapping, Wuhan University, Wuhan* 430079, *China*

[2] *Wuhan University's Key Antarctic Science Laboratory of SBSM, Wuhan* 430079, *China*

Abstract: A permanent tidal station was installed at the Chinese Zhongshan Station in Feb. 2010. Harmonic constants of 170 tidal constituents were obtained from harmonic analysis of the first year's data. The results of the eight main constituents showed good agreement with those of two tidal models. Tidal characteristics, such as tide type, diurnal inequality, tidal range, and water levels were also analyzed.

Key words: tidal characteristics; harmonic constants; tidal models; sea level; Antarctica

1 Introduction

Tidal data is essential for studying sea-level change[1-6], which is one of the most important consequences of global climate change; it is also vital for modeling the global ocean tides[7], which plays a key role in geophysical corrections for the satellite-altimetry sea level[8]. There are few tide-gauge stations in the southern ocean around Antarctica. Long-duration tide measurements in critical data-sparse areas are required to improve the performance of the data-assimilation model[9]. Few studies have been done because of the lack of tide data in Antarctica. Sun[10] analyzed tidal characteristics of the Great Wall Station at the King George Island, West Antarctica based on one-year tide data from March 1987 to February 1988.

This study focuses on the tide characteristics of Prydz Bay, based on the 365-day tide gauge data recorded from March 1, 2010 to February 28, 2011.

Received:2012-12-06; Accepted:2013-01-08

Corresponding author: Huang Jifeng, E-mail: huangjifeng@whu.edu.cn

This work is Supported by National Major Scientific Research Projects (2012CB957701), Natural Natural Science Foundation (41176172, 41176173, 41076126, 41106163), Polar Environment Comprehensive Expedition and the Resources Potential Evaluation Project (CHINARE 2012-01-03, CHINARE2012-02-02, CHINARE2012-03-03).

2 Data source and pre-processing

A permanent tide gauge station was installed at the Chinese Zhongshan Station in Prydz Bay, East Antarctica in February, 2010[11]. The location of the tide gauge, 69°22′11.5″S and 76° 22′19.4″ E(Fig. 1), was carefully selected to avoid moving icebergs and for convenient access to power supply. The instrument was a bottom-pressure tide gauge supplied by the Aanderaa company, which had three transducers to measure pressure(P), temperature(T) and conductivity(C), respectively. The sampling interval was set at one minute. As shown in table 1, there were five channels in the gauge to output raw data, which were five integers $N1$ – $N5$. $N1$ shows whether the gauge was working well (value 207 means the data is valid); $N2$ presented water temperature T; $N3$ and $N4$ could be converted to total pressure P, and conductivity C may be calculated from $N5$. The uniform formula for the calculation of the three parameters was

$$Y = A + BN + CN^2 + DN^3 \quad (1)$$

in which Y presents P, T, C, respectively, N presents

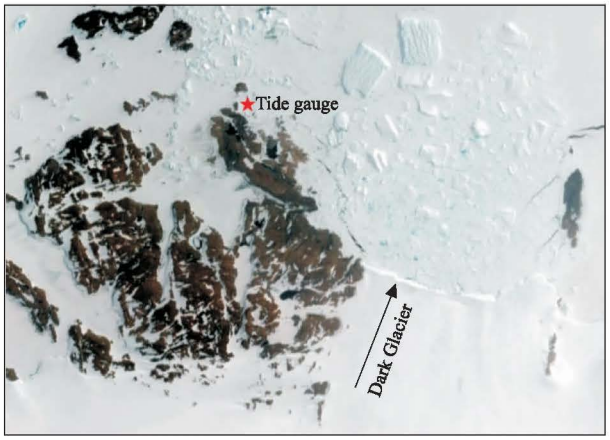

Figure 1 Asterisk shows the location of the Zhongshan Station in Prydz Bay, East Antarctica

N_2, N_p, N_5, respectively, N_p should be calculated from $N3$ and $N4$ by formula (2). The coefficients A, B, C, and D for each element are list in table 2.

$$N_p = N3 \times 1024 + N4 \tag{2}$$

Additional processing was needed to obtain the true sea-level height from the measured parameters (P, T, C). The conductivity was converted to salinity first and then the density of sea water ρ was calculated by the seawater state equation[12]. The sea level height was finally calculated by the hydraulic formula

$$h = \frac{(P - P_a)}{\rho G} \tag{3}$$

in which P is the total pressure, P_a is air pressure at mean sea level recorded by the meteorological station at Zhongshan Station, ρ is the density of sea water, G, whose value is 9.82572573 m/s^2, is the gravity acceleration of Zhongshan Station measured by absolute gravity measurement. The precision of the tide height was approximately better than two millimeters because the pressure sensor's calibration accuracy was 0.02% of full scale, which is always less than 6 meters.

The calculated sea-level-height data were carefully checked before further analysis. Abnormal fluctuation were found during 12 days in the analyzed time domain, which must be deleted for this study. Figure 2 shows the fluctuation (left) and the result after deleting the abnormal measurements (right) on June 23, 2010, as an example. This kind of abnormality may possibly have been caused by the tsunami as a result of an earthquake or certain iceberg input to the sea from the Dark Glacier 4 km to the southeast of Zhongshan Station (Fig. 1).

Table 1 Raw data from tide-gauge and sea-level height values

Time (yy-mm-dd Thh: mm)	$N1$	$N2$	$N3$	$N4$	$N5$	T(℃)	C (mmho/cm)	P (kPa)	SL (m)
2010-03-19T00 : 00	207	35	666	488	366	−1.78987	26.27634	145.4771	4.461
2010-03-19T00 : 01	207	34	666	472	366	−1.82572	26.27634	145.3853	4.453
2010-03-19T00 : 02	207	34	666	476	367	−1.82572	26.34933	145.4082	4.455
2010-03-19T00 : 03	207	34	666	485	366	−1.82572	26.27634	145.4599	4.460
2010-03-19T00 : 04	207	34	666	455	367	−1.82572	26.34933	145.2877	4.443

Table 2 Coefficients in equation (1) according to the gauge-calibration sheet

Y	A	B	C	D
Temperature	−3.054	3.641×10^{-2}	-8.746×10^{-6}	1.149×10^{-8}
Pressure	-4.779189×10^{3}	8.653580×10^{-3}	$-2.052078 \times 10^{-}9$	$-7.980398 \times 10^{-17}$
Conductivity	-4.380×10^{-1}	7.299×10^{-2}	0	0

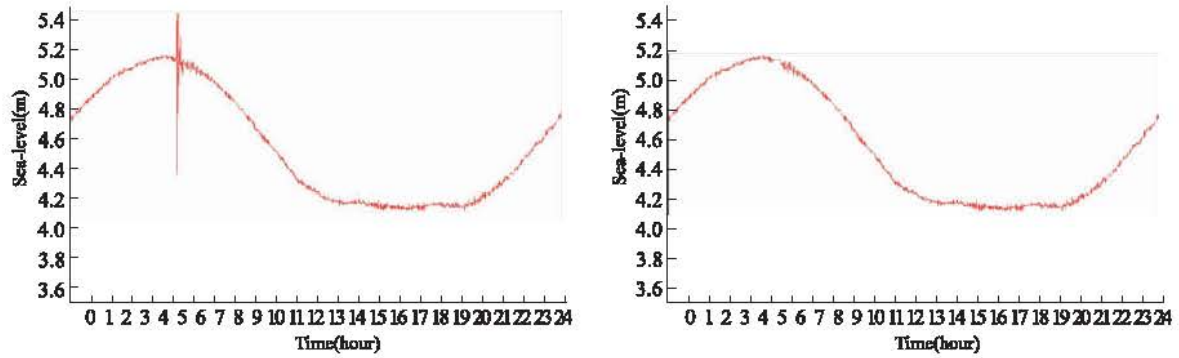

Figure 2 Fluctuations in raw sea-level data on June 23, 2010 (left), and after deletion (right).

3 Results

3.1 Tide models of the Southern Ocean

Several models of tides have been developed for the Southern Ocean, and they become more and more precise because data-assimilation approach has been adopted. Padman et al [9] described a model which used data assimilation to improve its fit to available data for the seas surrounding Antarctica. In 2005 King and Padman [13] presented an precision assessments for the tide models and concluded that the optimum tide model for Antarctica was TPXO6.2, which had been updated to TPXO7.2 recently (http://volkov.oce.orst.edu/tides/global.html). To take a look at the ocean tide in the Southern Ocean, we calculated the harmonic constants for the entire circum-Antarctic seas to 40°S at a resolution of 0.5° × 0.5°. Figure 3 shows the map of the sea-surface-height amplitude (m) of the four main constituents M2, S2, K1, O1 from model TPXO7.2. As shown in figure 3, there was a M2 amphidromic point (−66°30′, 58°16′) to the west of Zhongshan Station.

We also calculated the RMS tide height which is defined as the standard deviation of the modeled tidal-height fields summed over the eight main tidal constituents M2, S2, N2, K2, K1, O1, P1, and Q1. The ζ_σ value is given as a function of position (θ,φ) by

$$\zeta_\sigma(\theta,\varphi)=\sqrt{\sum_{n=1}^{8}H_n{}^2(\theta,\varphi)} \qquad (4)$$

where H_n is the height amplitude of the nth tidal coefficient. The map of RMS-tide height is plotted in figure 4. The RMS-tide height for Zhongshan Station was 0.500 m.

3.2 Harmonic constants

The harmonic constants of the main tidal constituents and the type of tide at Zhongshan Station have been reported by Huang Jifeng et al [11]. In this paper, all the harmonic constants of 170 constituents obtained by harmonic analysis of the first year's data are list in table 3.

The calculated harmonic constants of the eight main constituents were compared with those from two tidal models TPXO7.2 and CADA10. Good agreement between measured results and the models can be seen in table 4. The difference of amplitude ranges from 0.1 cm to 0.8 cm and 0.1 cm to 1.8 cm for TPXO and CADA, respectively. The results show that TPXO works a little better than CADA in Prydz Bay. Not only the tide-gauge data could be used to validate the tide models, but also the measured results could be assimilated into the tidal models to improve their precision[9], which may contribute to a range of precise satellite remote sensing missions [13].

The ratio of amplitude between main diurnal constituents and main semi-diurnal, $\frac{H_{K1}+H_{O1}}{H_{M2}}$, is 2.78, which indicates that the tide type of Zhongshan Station was irregular diurnal tide according to Chinese criterion for tide type determination [14]. Any day that has two high-low tides and one tide ranges being much smaller than any other one is considered as diurnal-tide day. The tide types are listed in table 5, which shows that May and January had the most number of diurnal-tide

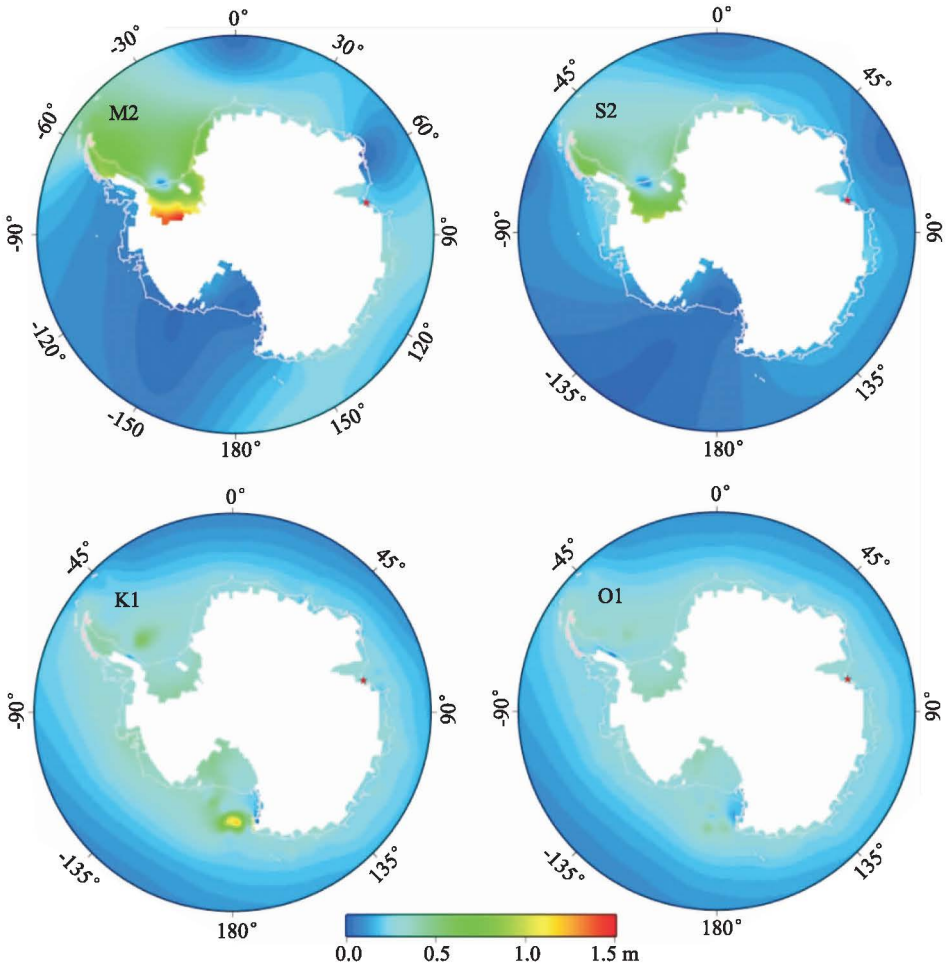

Figure 3 Maps of sea-surface-height amplitude (m) of M2, S2, K1, O1 from TPXO7.2. Asterisk indicates the tide-gauge location in Prydz Bay, East Antarctica

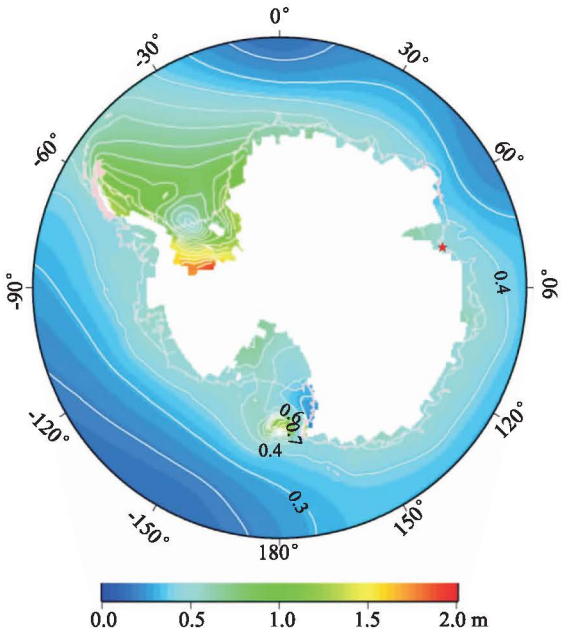

Figure 4 RMS tide height (ζ_σ) for Southern Ocean. The value near Zhongshan Station is approximately 0.5

days, whereas March and August had the least. There were 237 days which are diurnal-tide days in the whole year, about 65% of the total.

3.3 Diurnal inequality

There were 240 days that had two high-low tides, but only 84 days might be regarded as semi-diurnal tide days (table 5). This is because diurnal inequality was more noticeable. According to the calculated harmonic constants, the phase difference between the main diurnal constituent K1 and the main semi-diurnal constituent M2 is 193° and 159°for O1 and M2, respectively. As shown in figure 5, the inequality grows as the lunar declination increases, and this is noticeable for both high tide and low tide.

Table 3 The harmonic constants of 170 constituents from harmonic analysis of the first year's data

No.	Constituent	Amplitude (cm)	Phase (deg.)	No.	Constituent	Amplitude (cm)	Phase (deg.)
1	Sa	9.71	41.9	45	MNS_2	0.56	59.7
2	Ssa	4.91	344.4	46	$MNK2S_2$	0.36	38.4
3	(3)	5.7	53	47	$2MS2K_2$	0.06	19.6
4	(4)	24.32	299.8	48	$2N_2$	1.37	107.8
5	Mm	21.29	332.8	49	μ_2	1.19	135.8
6	(6)	16.69	183.1	50	SNK_2	0.12	92.2
7	MS_f	1.18	151.1	51	NSa_-	0.39	94.3
8	M_f	3.24	222.7	52	N_2	6.14	138.7
9	(9)	6.61	73	53	NSa_+	0.53	101.9
10	Mn	7.01	92.9	54	ν_2	1.74	138.8
11	(11)	0.24	60.7	55	$2KN2S_2$	0.26	142.8
12	(12)	1.23	30	56	OP_2	0.21	87.3
13	(13)	3.68	80.7	57	MSa_-	0.14	258
14	(14)	4.49	191.9	58	M_2	20.1	186.4
15	$2Q_1$	1.58	199.7	59	MSa_2	0.08	300
16	σ_{11}	1.21	205.6	60	MKS_2	0.21	302.3
17	Q_1Sa_-	0.81	191.6	61	$M2(KS)_2$	0.13	292.5
18	Q_1	7.33	217.9	62	$2SN(MK)_2$	0.25	188.3
19	Q_1Sa_+	1.18	182.4	63	λ_2	0.09	298.2
20	ρ_{11}	2.49	226.8	64	L_2	1.33	275.4
21	O_1Ssa_-	0.24	100.6	65	$2SK_2$	0.18	339.2
22	O_1Sa_-	0.53	118.2	66	T_2	1.6	292.5
23	O_1	28.34	245.7	67	S_2	18.08	312.5
24	O_1Sa_+	0.23	296.4	68	R_2	0.1	221.2
25	MP_1	0.35	234.5	69	K_2	5.05	317.7
26	ν_1	0.52	113.3	70	MSN_2	0.36	342.6
27	M_1	1.96	5.4	71	KJ_2	0.69	185.6
28	χ_1	0.78	185.7	72	$2KM(SN)_2$	0.29	7.5
29	π_1	0.59	299.2	73	$2SM_2$	0.29	32.9
30	P_1	8.68	277.1	74	SKM_2	0.24	59.8
31	S_1	1.07	260.1	75	$2SN_2$	0.35	72.2
32	K_1	27.51	279.5	76	SKN_2	0.34	87.3
33	ψ_1	0.11	77.4	77	MQ_3	0.26	98.1
34	φ_1	0.6	270.2	78	MO_3	0.43	281.4
35	θ_1	0.67	232	79	$2MP_3$	0.27	85.6
36	J_1	1.71	281.5	80	M_3	1.53	227.1
37	$2PO_1$	0.12	193.3	81	SO_3	0.23	325.2
38	SO_1	0.36	316.2	82	MK_3	0.42	133.4
39	OO_1	0.59	299	83	$2MQ_3$	0.42	173.5
40	KQ_1	0.72	1.3	84	SP_3	1.06	180.2
41	$2MN2S_2$	0.35	272.9	85	SK_3	0.94	207.7
42	$2NS_2$	0.33	39.2	86	K_3	0.14	222.9
43	$3M2S_2$	0.05	330.1	87	$2MNS_4$	0.13	287.6
44	OQ_2	0.34	204.3	88	$3MK_4$	0.06	61.8

Table 3 Continued

No.	Constituent	Amplitude (cm)	Phase (deg.)	No.	Constituent	Amplitude (cm)	Phase (deg.)
89	$3MS_4$	0.1	81.2	131	$2SN_6$	0.08	119.9
90	$MSNK_4$	0.11	353.7	132	NSK_6	0.16	109.9
91	MN_4	0.27	13.2	133	MKL_6	0.23	333
92	$M\nu_4$	0.25	49	134	$2SM_6$	0.12	298.8
93	$2MSK_4$	0.19	338.1	135	MSK_6	0.13	296.3
94	M_4	0.25	124.8	136	S_6	0.15	103.8
95	$2MKS_4$	0.14	186.7	137	$2SK_6$	0.32	346
96	SN_4	0.18	104.2	138	$2MNO_7$	0.02	35
97	$3MN_4$	0.18	145.2	139	$2NMK_7$	0.1	212.2
98	$2SMK_4$	0.09	253.8	140	M_7	0.05	293.2
99	MT_4	0.13	176.2	141	$2MSO_7$	0.08	157.3
100	MS_4	0.12	223.2	142	$MSKO_7$	0.09	267.8
101	MK_4	0.13	281.5	143	$2(MN)_8$	0.11	201.4
102	$2SNM_4$	0.13	195.5	144	$3MN_8$	0.03	102
103	$2MSN_4$	0.19	240.6	145	$3MNKS_8$	0.01	235
104	S_4	0.12	333.3	146	M_8	0.06	4.4
105	SK_4	0.08	339.1	147	$2MSN_8$	0.04	245
106	$2SMN_4$	0.17	332.6	148	$2MNK_8$	0.04	310.4
107	$3SM_4$	0.11	96.3	149	$3MS_8$	0.07	67.1
108	$2SKM_4$	0.09	100.5	150	$3MK_8$	0.06	95
109	MNO_5	0.06	335.6	151	$MSNK_8$	0.02	53
110	$2MO_5$	0.09	173.8	152	$2(MS)_8$	0.09	156.5
111	$3MP_5$	0.13	345.9	153	$2MSK_8$	0.08	195.3
112	M_5	0.11	44.5	154	$2M2NK_9$	0.07	131.4
113	$2MP_5$	0.09	251.2	155	$3MNK_9$	0.03	17.4
114	$2MK_5$	0.09	86.7	156	$4MK_9$	0.1	273
115	MSK_5	0.06	220.3	157	$3MSK_9$	0.11	348.2
116	KKM_5	0.09	182.8	158	$4MN_{10}$	0.06	228.4
117	$2(MN)S_6$	0.16	200.4	159	M_{10}	0.12	246.9
118	$3NKS_6$	0.04	15.1	160	$3MNS_{10}$	0.02	314.6
119	$2NM_6$	0.19	304.6	161	$4MS_{10}$	0.14	355.9
120	$2NMKS_6$	0.09	334.4	162	$2(MS)N_{10}$	0.03	147.1
121	$2MSNK_6$	0.13	238.2	163	$2MNSK_{10}$	0.02	121.8
122	$2MN_6$	0.21	8.5	164	$3M2S_{10}$	0.11	79.5
123	$2MNKS_6$	0.07	284	165	$4MSK_{11}$	0.1	265.6
124	$3MSK_6$	0.08	32.5	166	M_{12}	0.12	141.3
125	M_6	0.55	98.9	167	$4MNS_{12}$	0.04	242.4
126	MSN_6	0.05	77.1	168	$5MS_{12}$	0.07	257.5
127	MKN_6	0.07	285.3	169	$3MNKS_{12}$	0.03	334.5
128	$MK\nu_6$	0.1	56	170	$4M2S_{12}$	0.1	357.5
129	$2MS_6$	0.47	225.5				

Table 4 Comparison of the harmonic constants between the models and the measured results

Harmonic constants		M2	S2	N2	K2	K1	O1	P1	Q1
Amplitude (cm)	Measured	20.1	18.1	6.1	5.1	27.5	28.3	8.7	7.3
	TPXO7.2	20.3	17.8	6.6	5.8	28	28.2	8.6	6.5
	CADA10	19.0	18.0	6.4	5.7	26.0	27.7	10.5	7.9
	TPXO – measured	0.2	−0.3	0.5	0.7	0.5	−0.1	−0.1	−0.8
	CADA – measured	−1.1	−0.1	0.3	0.6	−1.5	−0.6	1.8	0.6
Phase (deg.)	Measured	186.4	312.5	138.7	317.7	279.5	245.7	277.1	217.9
	TPXO7.2	210.7	315.3	174.3	310.8	281.3	269	282.2	261.6
	CADA10	216.1	324.6	173	320.6	286	276	277	257
	TPXO – measured	24.3	2.8	35.6	−6.9	1.8	23.3	5.1	43.7
	CADA – measured	29.7	12.1	34.3	2.9	6.5	30.3	−0.1	39.1

Table 5 Tidal type of each month

Year	2010										2011		Average	Total
Month	3	4	5	6	7	8	9	10	11	12	1	2		
Semi-diurnal tide	13	4	3	4	9	8	10	4	7	5	8	9	7	84
Diurnal tide	16	22	24	20	19	15	17	21	22	22	23	16	20	237
Interim	2	4	4	6	3	8	3	6	1	4	0	3	4	44

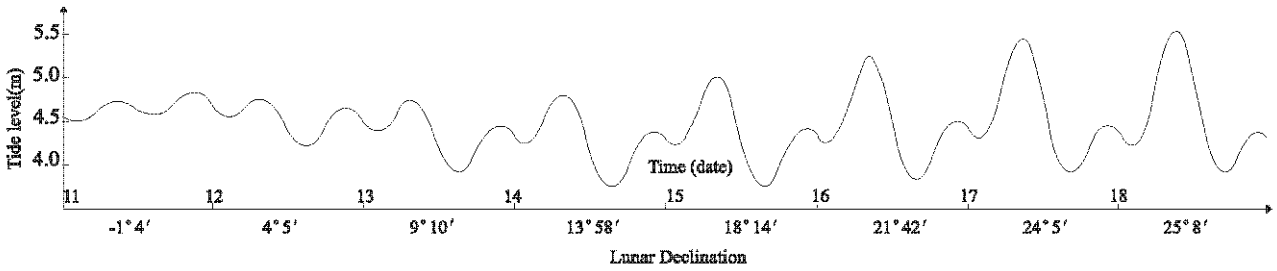

Figure 5 Tide curve during April 11 – 18, 2010

Table 6 Monthly average duration of rising and falling tide (Unit: hour)

Year	2010										2011		Average
Month	3	4	5	6	7	8	9	10	11	12	1	2	
Duration of rising tide	6.24	6.65	8.61	8.26	7.90	7.25	6.72	6.37	7.92	8.05	8.24	7.16	7.37
Duration of falling tide	7.03	6.68	6.91	7.77	8.13	7.65	7.40	6.47	6.77	7.71	8.27	7.80	7.34
Rising – falling	−47	−2	102	29	−14	−24	−41	−6	69	20	−2	−38	2

3.4 Duration of rising and falling tide

The average duration of rising tide was 7 hours and 22 minutes, whereas that of falling tide was 7 hours and 20 minutes, with a 2-minute difference. As shown in table 6, the four months of rising tide being longer than that of falling tide were May, June, November and December. The maximum difference between rising and falling duration occurred in May, and it is 1 hour and 42 minutes.

3.5 Tidal range

Tidal range is one of the most important characteristics, which may indicate the tide strength in the study

area.

3.5.1 Average tide range

In Prydz Bay, the average tidal range in the study period was 0.799 m. The maximum monthly average tide range was 0.94 m in January and the minimum was 0.666 m in October, the difference being 0.274 m. Figure 6 shows the seasonal variation of the observed tide range. We can see that the monthly average tide range was bimodal with two maxima in July and January and two minima in April and October.

3.5.2 Maximum tide range

The two monthly maximum tide ranges were 1.839 m in May and 1.694 m in October.

As shown in figure 6, the monthly maximum tide-range curve was also bimodal, with two maxima in May and October and two minima in August and January, being in opposite phase to the monthly average-tide range.

3.6 Water levels

3.6.1 Average water level

In the study period, the yearly average sea level was 4.466 m. The monthly average water level showed a remarkable seasonal variation. The maximum monthly average water level was 4.578 m in June and the minimum is 4.386 m in November, the difference being 0.192 m. As shown in figure 7, the monthly average water level in the winter half year (from May to October) was 4.497 m, which was 0.062 m higher than that of the summer half year (from November to April) 4.435 m. The amplitude of the variation in the winter half year was 0.159 m, which was 0.064 m more than that of the summer half year (0.095 m).

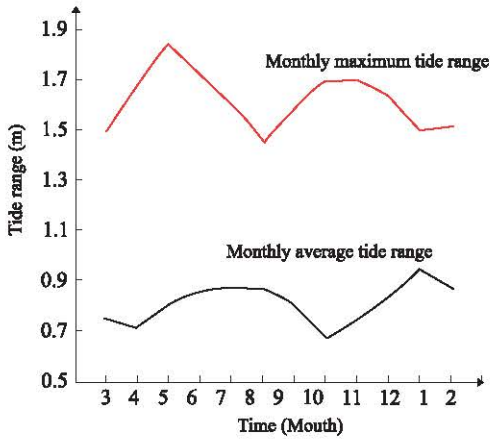

Figure 6 Seasonal variability of the tidal range form 2010 to 2011

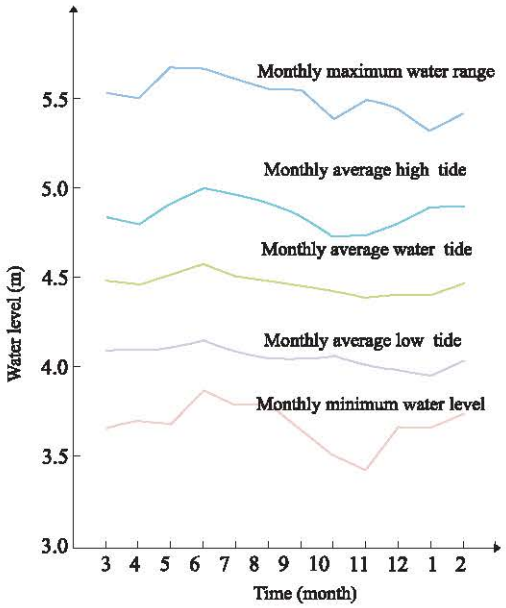

Figure 7 Seasonal variation of water levels in the study period from 2010 to 2011

3.6.2 Average high and low tides

The yearly average high tide was 4.865 m, which was 0.399 m higher than the yearly average sea level, and the yearly average low tide was 4.057 m, which was 0.409 m lower than the yearly average sea level. The maximum monthly average high tide was 5.001 m in June and the minimum was 4.735 m in October, the difference being 0.266 m.

The maximum monthly average low tide was 4.152 m in June and the minimum was 3.955 m in January, the difference being 0.197 m.

3.6.3 Extremum sea levels

The maximum sea level was 5.680 m, which occurred at 08 : 39 on May 16, 2010, and the minimum was 3.422 m at 02 : 53 on November 6, 2010, with a height difference of 2.258 m.

4 Conclusions

1) The harmonic constants calculated from the tide gauge measurements are important to validate available tidal models, and they can also be assimilated into the models to improve their accuracy.

2) The tide type at the Zhongshan Station in Prydz Bay was irregular diurnal tide.

3) There is a notable tide inequality; and the inequalities of both high tide and low tide were remarkable.

4) Although a difference between the annual average duration of rising and falling tide was negligible, the monthly average duration difference showed clear variations with two maxima in May and November and two minima in March and September, being highly correlated with the diurnal-tide days during each month.

5) The annual average tide range was 0.799 m and the maximum was 1.839 m during the study period.

6) The annual average sea level was 4.466 m. The maximum was 5.680 m at 08 : 39 on May 16, 2010 and the minimum was 3.422 m at 02 : 53 on November 6, 2010, with a height difference of 2.258 m. Compared with the summer half year, the average water level in the winter half year was higher with larger variation.

Acknowledgment

We thank the expedition crew members of CHINARE 26 for their help in the field work.

References

[1] Tai C K. Inferring the global mean sea level from a global tide gauge network. Acta Oceanologica Sinica, 2011, 30(4): 102 - 6.

[2] Wöppelmann G and Marcos M. Coastal sea level rise in southern Europe and the nonclimate contribution of vertical land motion. J Geophys Res., 2012, 117(C1): C01007.

[3] King M A, Keshin M, Whitehouse P L, Thomas, Ian D, Milne Glenn and Riva Riccardo E M. Regional biases in absolute sea-level estimates from tide gauge data due to residual unmodeled vertical land movement. Geophys Res Lett., 2012, 39(14): L14604.

[4] Houston J R and Dean R G. Sea-level acceleration based on US tide gauges and extensions of previous global-gauge analyses. Journal of Coastal Research, 2011, 27(3): 409 - 17.

[5] Marcos M, Puyol B, Wöppelmann G, Herrero Carmen and García-Fernández M Jesús. The long sea level record at Cadiz (southern Spain) from 1880 to 2009. J Geophys Res., 2011, 116(C12): C12003.

[6] Trisirisatayawong I, Naeije M, Simons W and Fenoglio-Marc L. Sea level change in the Gulf of Thailand from GPS-corrected tide gauge data and multi-satellite altimetry. Global and Planetary Change, 2011, 76(3 - 4): 137 - 51.

[7] Florent L, Fabien L, Thierry L and Olivier Francis. Modelling the global ocean tides: modern insights from FES2004. Ocean Dynamics, 2006, 56(5 - 6): 394 - 415.

[8] Ablain M, Cazenave A, Valladeau G and Guinehut S. A new assessment of the error budget of global mean sea level rate estimated by satellite altimetry over 1993 - 2008. Ocean Science, 2009, 5(2): 193 - 201.

[9] Padman L, Fricker H A, Coleman R, Howard S and Erofeeva L. A new tide model for the Antarctic ice shelves and seas. Annals of Glaciology. 2002, 34(1): 247 - 54.

[10] Sun Hongliang. The tidal characteristics and the meteorological influence on the mean sea level at the Great Wall Station in West Antarctic. Acta Oceanologica Sinica, 1992, 14(4): 112 - 23. (in Chinese)

[11] Huang Jifeng, E Dongchen, Zhang Shengkai and Zhou Chunxia. Processing and analysis of tidal data For Zhongshan Station, East Antarctic. Journal of Geodesy and Geodynamics, 2012, 32(5): 63 - 7. (in Chinese)

[12] Fofonoff N P and Millard R C. Algorithms for computation of fundamental properties of seawater. Paris: Unesco, 1983.

[13] King M A and Padman L. Accuracy assessment of ocean tide models around Antarctica. Geophysical Research Letters, 2005, 32(23): L23608.

[14] Huang Zuke and Huang Lei. Tide height for Engineering. Tidal Theory and Calculation. Qingdao: Ocean University of China Press, 2005. (in Chinese)